Thermodynamic constraints on the regulation of metabolic fluxes

Received for publication, June 9, 2018, and in revised form, September 17, 2018 Published, Papers in Press, October 25, 2018, DOI 10.1074/jbc.RA118.004372

Ziwei Dai[1] **and Jason W. Locasale**[2]

From the Department of Pharmacology and Cancer Biology, Duke University School of Medicine, Durham, North Carolina 27710

Edited by John M. Denu

Nutrition and metabolism are fundamental to cellular function. Metabolic activity (*i.e.* rates of flow, most commonly referred to as flux) is constrained by thermodynamics and regulated by the activity of enzymes. The general principles that relate biological and physical variables to metabolic control are incompletely understood. Using metabolic control analysis and computer simulations in several models of simplified metabolic pathways, we derive analytical expressions that define relationships between thermodynamics, enzyme activity, and flux control. The relationships are further analyzed in a mathematical model of glycolysis as an example of a complex biochemical pathway. We show that metabolic pathways that are very far from equilibrium are controlled by the activity of upstream enzymes. However, in general, regulation of metabolic fluxes by an enzyme has a more adaptable pattern, which relies more on distribution of free energy among reaction steps in the pathway than on the thermodynamic properties of the given enzyme. These findings show how the control of metabolic pathways is shaped by thermodynamic constraints of the given pathway.

Metabolism enables the utilization of nutritional resources to provide free energy, material, and cellular communication for functions of cells (1). Some metabolic pathways such as central carbon metabolism, which processes macronutrients or the major caloric sources in diet (proteins, fats, and carbohydrates), have been largely defined for over 50 years (2), and even genome-scale reconstructions of metabolic networks that include thousands of metabolites and reactions in different intracellular compartments are available in many unicellular organisms and metazoans (3–5). Despite the complexity of metabolic networks in living organisms, metabolic processes still follow the laws of thermodynamics. It is thus important to understand the principles that link fundamental thermodynamic quantities to the control of metabolic pathway activity (*i.e.* the rates of flow of materials through the network, most commonly referred to as fluxes).

Analytical frameworks have been developed to understand steady-state and dynamic behaviors of metabolic networks. The most widely applied method in computational modeling of metabolism is flux balance analysis, which assumes that the network is in steady state and that configurations of metabolic fluxes are determined by optimizing an objective function such as growth rate (6). This approach does not require that enzyme properties such as expression levels be known, but the utility of the method depends on the objective function and other assumptions such as nutrient uptake rates. Moreover, flux balance analysis does not provide information about pathway regulation and the control of metabolic flux, which requires additional knowledge such as enzyme activities or metabolite abundances, which are routinely measurable (7, 8).

Another framework for understanding metabolism is metabolic control analysis (MCA),[3] originally developed in the 1970s once the biochemistry for many of the key pathways in metabolism such as glycolysis and the tricarboxylic acid cycle was established (9–15). MCA quantitatively measures how the flow through a metabolic pathway responds to changes in parameters such as the abundance of an enzyme or availability of a nutrient. MCA defines the sensitivity of a metabolic flux to a perturbation in a given metabolic reaction (*i.e.* the flux control coefficients (FCCs)) and also provides a series of rigorously derived relationships between metabolic fluxes, metabolite concentrations, and enzyme activities. This framework can also be applied in computer simulations (16–19) or in experimentation (20, 21) when some but not all of the relevant variables are measured (22–25).

Metabolism is subject to the laws of thermodynamics. These laws place constraints on the dynamics of metabolic reactions (26–32) and are known to affect the control of fluxes in linear pathways (9, 31, 33, 34). Moreover, the deviation from equilibrium at an individual reaction step has been applied as the criterion to identify rate-limiting steps in metabolic pathways (2, 29). However, this rule of thumb has been challenged by MCA, at least for linear pathways (9), but a quantitative evaluation of the relationship between thermodynamics and flux control in metabolic pathways with different topologies such as the control at branching points is still lacking.

In this study, we use a set of models with representative topological structures observed in metabolism to investigate the quantitative relationships between thermodynamics and regulation of metabolic fluxes. Notably, all models are based on

This work was supported by National Institutes of Health Grants R01 CA193256 and R00CA168997 and American Cancer Society Grant TBE-TBE434120 (to J. W. L.). The authors declare that they have no conflicts of interest with the contents of this article. The content is solely the responsibility of the authors and does not necessarily represent the official views of the National Institutes of Health.

This article contains supporting information and Figs. S1 and S2.

[1] To whom correspondence may be addressed. E-mail: ziwei.dai@duke.edu.

[2] To whom correspondence may be addressed. E-mail: jason.locasale@duke.edu.

[3] The abbreviations used are: MCA, metabolic control analysis; FCC, flux control coefficient; TDF, thermodynamic driving force.

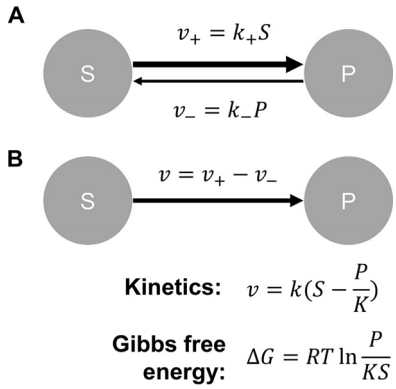

Figure 1. First-order kinetics of enzyme-catalyzed reversible reactions. *A*, forward and backward fluxes of a reversible reaction. *S* is the concentration of substrate, *P* is the concentration of product, v_+ is the rate of the forward reaction, v_- is the rate of the backward reaction, k_+ is the rate constant of the forward reaction, and k_- is the rate constant of the backward reaction. *B*, net flux and Gibbs free energy change of a reversible reaction. *v* is the net reaction rate, *k* is the rate constant, *K* is the equilibrium constant, ΔG is the reaction Gibbs free energy change, *R* is the universal gas constant, and *T* is the temperature. Other variables are the same as in *A*.

some simplifying assumptions, but some (and hopefully these) are useful. To our surprise, we find that, in both linear and branched pathways, the regulation of pathway fluxes by individual enzymes is in general loosely constrained by the deviation from thermodynamic equilibrium, or the thermodynamic driving force, of the whole pathway. Only pathways very far from equilibrium have their flux regulation strictly constrained by the thermodynamic driving force, in which all fluxes are almost fully controlled by the upstream enzymes. The relationships are further studied in a mathematical model of glycolysis as an example of a more complicated metabolic model. These results unravel simple principles of how metabolic pathways are regulated by the interaction between thermodynamics and enzyme activity.

Results

Metabolic flux and thermodynamics

We first consider unimolecular, first-order kinetics of reversible metabolic reactions for simplicity. In this framework, each reaction has one substrate (*S*) and one product (*P*) (Fig. 1). It is noteworthy that this simplified case approximates the more complicated Michaelis–Menten mechanism when the abundance of substrate is far below the K_m. The forward reaction rate $v_+ = k_+S$ and backward reaction rate $v_- = k_-P$ are linear in substrate and product concentrations. Because the rate constants of the forward and backward reactions are coupled by the equilibrium constant K:$K = k_+/k_-$, the net flux carried by this reaction is as follows: $v = v_+ - v_- = k_+(S - P/K)$. Let $k = k_+$ for simplicity, and we have the following.

$$v = k\left(S - \frac{P}{K}\right) \qquad \text{(Eq. 1.1)}$$

The equilibrium constant *K* can be further connected to the standard Gibbs free energy of this reaction.

$$\Delta G^\circ = -RT \ln K \qquad \text{(Eq. 1.2)}$$

Finally, the Gibbs free energy is determined by the standard Gibbs free energy in combination with concentrations of the substrate and product.

$$\Delta G = \Delta G^\circ + RT \ln \frac{P}{S} = RT \ln \frac{P}{KS} \qquad \text{(Eq. 1.3)}$$

We note that Equation 1.1 can also be rewritten to explicitly incorporate the reaction free energy change. Here, we let $g = \Delta G/RT$ for simplicity. Thus, we have the following.

$$v = kS(1 - e^g) = \frac{kP}{K}(e^{-g} - 1) \qquad \text{(Eq. 1.4)}$$

According to the connectivity theorem in MCA (13), flux control coefficients of reactions directly associated with a metabolite are coupled through local elasticity coefficients of these reactions with respect to the metabolite. For a reaction and a metabolite directly associated with this reaction (either as substrate or as product), the elasticity coefficient is defined as the partial derivative of the reaction rate with respect to the concentration of the metabolite on the logarithmic scale. The elasticity coefficients can be computed from Equations 1.1 and 1.4.

$$\begin{cases} \varepsilon_S = \dfrac{S}{v}\dfrac{\partial v}{\partial S} = \dfrac{S}{S - \dfrac{P}{K}} = \dfrac{1}{1 - e^g} \\ \varepsilon_P = \dfrac{P}{v}\dfrac{\partial v}{\partial P} = \dfrac{P}{P - KS} = \dfrac{1}{1 - e^{-g}} \end{cases} \qquad \text{(Eq. 1.5)}$$

Linear pathways

Based on the definitions under "Metabolic flux and thermodynamics," we now consider a linear pathway consisting of *n* reactions (Fig. 2*A*). Each reaction has unimolecular, linear kinetics, as described previously. The first substrate S_{in} is converted to the end product S_{out} by this reaction chain in *n* steps with $n - 1$ intermediary metabolites $S_1, \ldots, S_{n-1}$. The *i*th reaction in this chain has rate constant k_i and equilibrium constant K_i. The concentrations of S_{in} and S_{out} are treated as fixed parameters, because these two values, together with rate constants and equilibrium constants of the enzymes, determine concentrations of all other metabolites.

Previous work has shown that in linear pathways with either first-order or zero-order (*i.e.* substrate-saturated) kinetics, the pattern of flux control can be completely determined if free energies of all reactions involved in the pathway are known (34). Here, we use these results as necessary background to study the relationship between thermodynamics and flux control in metabolic networks with different topological structures. Briefly, from MCA (13), there are analytical relationships between thermodynamic properties and the flux control coefficients, which quantify the relative importance of each enzyme in regulating the flux through the pathway.

To apply the summation theorem and connectivity theorems in the theory of metabolic control analysis, we assume that the

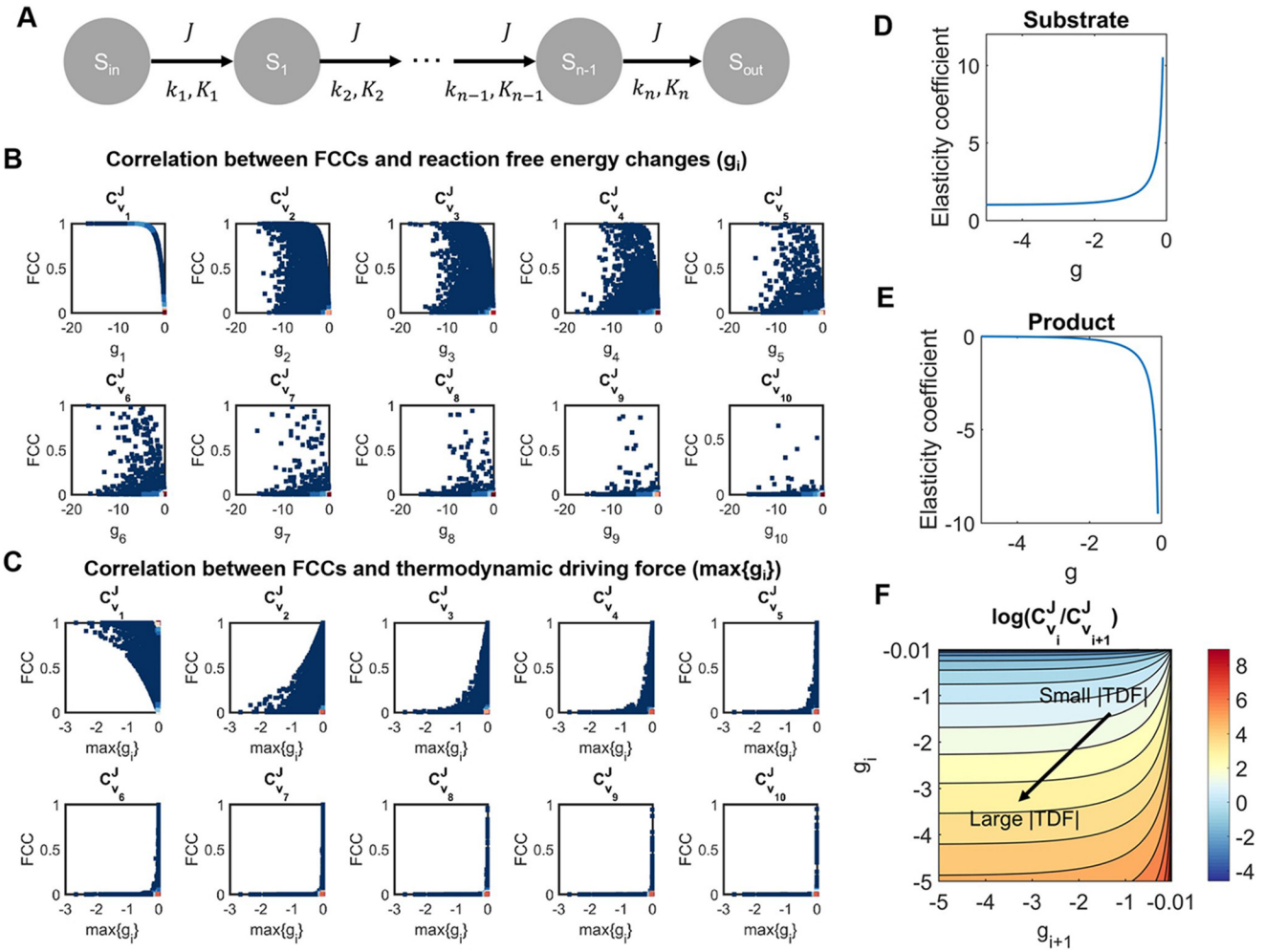

Figure 2. Thermodynamics and flux regulation in a linear pathway. *A*, diagram of a linear pathway and related parameters. S_{in} is the input substrate, S_{out} is the final product, S_i is the *i*th intermediary metabolite, k_i is the rate constant of the *i*th reaction, K_i is the equilibrium constant of the *i*th reaction, and *J* is the pathway flux. *B*, scatter plots comparing flux control coefficients and reaction free energy changes in a linear pathway with randomly sampled parameters. The pathway includes 10 reaction steps. C^J_{vi} is the *i*th flux control coefficient, and $g_i = \Delta G_i/RT$ quantifies the *i*th free energy change. *C*, scatter plots comparing flux control coefficients and the thermodynamic driving force (max{g_i}) in a linear pathway with randomly sampled parameters. Variables are the same as in *B*. *D*, relationship between free energy of a reaction and the elasticity coefficient of its velocity toward the substrate. *E*, relationship between free energy of a reaction and the elasticity coefficient of its velocity toward the product. *F*, relationship between the free energies of two sequential reactions and the ratio of the flux control coefficients associated with the two reactions.

pathway is in steady state, in which all reactions have identical net flux. In other words, all intermediary metabolites have balanced fluxes feeding and consuming them. Thus, we can write $n - 1$ equations for the steady-state constraints.

$$k_{i-1}\left(S_{i-2} - \frac{S_{i-1}}{K_{i-1}}\right) = k_i\left(S_{i-1} - \frac{S_i}{K_i}\right) \qquad \text{(Eq. 2.1)}$$

Let *J* denote the net flux through this pathway. The flux control coefficient, C^J_{vi}, quantifies the sensitivity of the pathway flux *J* to perturbation in activity (*i.e.* rate constant) of the *i*th reaction. It is defined as the ratio of relative change in the flux *J* to relative change in the rate of the *i*th reaction when an arbitrary parameter *p* that only affects the rate of the *i*th reaction and no other reactions has a small change.

$$C^J_{v_i} = \frac{\partial \log J/\partial \log p}{\partial \log v_i/\partial \log p} \qquad \text{(Eq. 2.2)}$$

If $p = k_i$, we have the following.

$$C^J_{v_i} = \frac{k_i}{J}\frac{\partial J}{\partial k_i} \qquad \text{(Eq. 2.3)}$$

The flux control coefficients can be uniquely determined by solving equations derived from the summation and connectivity theorems. For linear pathways, the summation and connectivity theorems do not explicitly include the pathway flux *J*.

Summation theorem

$$\sum_{i=1}^{n} C^J_{v_i} = 1 \qquad \text{(Eq. 2.4)}$$

Connectivity theorem

$$C^J_{v_i}\epsilon^{v_i}_{S_{i-1}} + C^J_{v_{i-1}}\epsilon^{v_{i-1}}_{S_{i-1}} = 0 \qquad \text{(Eq. 2.5)}$$

According to Equation 1.5, we have the following.

$$\begin{cases} \varepsilon_{S_{i-1}}^{v_{i-1}} = \dfrac{S_{i-1}}{S_{i-1} - K_{i-1}S_{i-2}} = \dfrac{1}{1-e^{-g_{i-1}}} \\ \varepsilon_{S_{i-1}}^{v_i} = \dfrac{S_{i-1}}{S_{i-1} - \dfrac{S_i}{K_i}} = \dfrac{1}{1-e^{g_i}} \end{cases} \quad \text{(Eq. 2.6)}$$

Flux control coefficients can be solved by combining Equations 2.1, 2.4, 2.5, and 2.6 (see supporting information). They can be written as either explicitly including only the reaction free energy terms or explicitly including only the rate constants and equilibrium constants.

$$C_{v_i}^J = \frac{1-e^{g_i}}{1-\prod_{l=1}^{n} e^{g_l}} \prod_{m=1}^{i-1} e^{g_m} \quad \text{(Eq. 2.7)}$$

$$C_{v_i}^J = \frac{1}{k_i \prod_{l=1}^{i-1} K_l \left(\sum_{l=1}^{n} \frac{1}{k_l \prod_{m=1}^{l-1} K_m} \right)} \quad \text{(Eq. 2.8)}$$

According to Equations 2.7 and 2.8, the flux control coefficients are completely determined by kinetic and thermodynamic parameters of reactions in the pathway. Therefore, alterations in concentrations of the input substrate and the final product do not influence the flux control coefficients.

To illustrate the quantitative relationships defined in Equations 2.7 and 2.8, we consider a linear pathway consisting of 10 reactions; randomly sample 20,000 combinations of the parameters S_{in}, S_{out}, $\{k_i\}$, and $\{K_i\}$; and compute the corresponding flux control coefficients. We select the size 10 because it approximates the typical length of linear metabolic pathways. All parameters and substrate concentrations are sampled from a log-normal distribution.

$$\log_{10}(k_i, K_i, S_{in}, S_{out}) \sim N(1,1), i = 1, 2, \ldots, 10 \quad \text{(Eq. 2.9)}$$

We first correlate the flux control coefficient with reaction free energy change for each individual reaction (Fig. 2*B*). We find that the relationship between reaction free energy changes and flux control coefficients calls into question the longstanding hypothesis that reactions with the most negative free energy changes, such as the reactions catalyzed by hexokinase, phosphofructokinase, and pyruvate kinase in glycolysis, serve as rate-limiting steps of a pathway (35–38). Although previous work in metabolic control analysis has provided the theoretical framework to study the role of thermodynamics in the regulation of metabolic fluxes (34), this hypothesis is still widely accepted (39–41). However, according to our analysis, for all reactions except the first reaction, their flux control coefficients correlate poorly with the reaction free energy changes, suggesting that a large absolute value of free energy change is dispensable for a rate-limiting step, and regulation of metabolic fluxes by an individual reaction is determined by both thermodynamics property and position along the pathway.

We next investigate how the flux control coefficients are associated with global thermodynamic properties of the entire pathway. We quantify the deviation from the thermodynamic equilibrium by the reaction free energy change that is closest to zero (*i.e.* the maximal value of free energy change among all reactions). When this quantity equals zero, the pathway has zero net flux (*i.e.* thermodynamic equilibrium). Moreover, when this quantity is close to zero, at least part of the pathway is not efficiently driven by thermodynamics, resulting in inefficient usage of enzymes with free energy changes close to zero (34). Thus, it is termed the thermodynamic driving force (TDF).

$$TDF = \max_i\{g_i\} \quad \text{(Eq. 2.10)}$$

We correlate the thermodynamic driving force with flux control coefficient of each reaction step (Fig. 2*C*). From these simulations, a pattern emerges, in which the thermodynamic driving force determines either the upper bound or lower bound of the flux control coefficients; for the flux control coefficient of the first reaction (C_{v1}^J), its lower bound depends on the thermodynamic driving force, whereas for the rest of the reactions, the upper bounds of their flux control coefficients depend on the thermodynamic driving force.

Analytical relationships that constrain flux control coefficients by thermodynamic driving force can also be derived from Equations 2.7 and 2.10 (see supporting information).

$$C_{v_i}^J > 1 - e^{TDF} \quad \text{(Eq. 2.11)}$$

$$C_{v_i}^J < \frac{e^{(i-1)TDF}}{1-e^{n(TDF)}} \quad \text{(Eq. 2.12)}$$

From Equations 2.11 and 2.12, we can derive corollary relationships for the flux control coefficients when the system is very far from equilibrium (*i.e.* thermodynamic driving force approaches minus infinity).

$$\lim_{TDF \to -\infty} C_{v_i}^J = \begin{cases} 1, & i = 1 \\ 0, & i > 1 \end{cases} \quad \text{(Eq. 2.13)}$$

Equation 2.13 suggests that in a linear pathway far from thermodynamic equilibrium, the metabolic flux through the pathway is fully controlled by the enzyme catalyzing the first step. In other situations when the thermodynamic driving force has a smaller absolute value, the flux control is more evenly distributed among all enzymes in the pathway.

An intuitive interpretation of the relationship between the thermodynamic driving force and flux control coefficients can be given based on the fact that for a reaction with first-order kinetics, the elasticity coefficients toward the sub-

strate and product can be completely determined if the free energy of this reaction is known (Fig. 2 (*D* and *E*) and Equation 2.6). According to the connectivity theorem (Equation 2.5), in a linear pathway, the ratio of the *i*th flux control coefficient to the $i + 1$th flux control coefficient can be written as a function of the free energies of the *i*th and i + 1*th* reactions (Fig. 2*F*).

$$\frac{C^J_{v_i}}{C^J_{v_{i+1}}} = -\frac{\epsilon^{v_{i+1}}_{S_i}}{\epsilon^{v_i}_{S_i}} = \frac{1 - e^{g_i}}{e^{g_i}(1 - e^{g_{i+1}})} \quad \text{(Eq. 2.14)}$$

Thus, the thermodynamic driving force constrains the distribution of flux control among enzymes by constraining the elasticity coefficients that determine flux control coefficients through the connectivity theorem. When the thermodynamic driving force has a large absolute value (*i.e.* TDF approaches minus infinity; *bottom left corner* in Fig. 2*F*), for any reaction in the pathway, its elasticity coefficient with respect to the product is very close to zero, which means that altering the concentration of the product has negligible influence on the rate of this reaction. In this situation, perturbation of any downstream enzyme has a minimal effect on the first reaction, whose rate is equal to the overall flux, because the effect must be propagated through the metabolite S_1, which serves as the product of the first reaction. On the other hand, when the thermodynamic driving force is close to zero (*top right corner* in Fig. 2*F*), the ratio between two sequential flux control coefficients is more flexible, resulting in what we term as a more adaptable pattern of flux control in these pathways.

To summarize, for a linear metabolic pathway with first-order kinetics, we have derived analytical relationships between the flux control coefficients and thermodynamic properties of both individual reactions and the entire pathway. We have shown that the flux control coefficients correlate poorly with free energy changes of the corresponding reactions but that the thermodynamic driving force of the whole pathway places bounds on how much any enzyme can control pathway flux. However, when the pathway is very far away from thermodynamic equilibrium, the metabolic flux through this pathway is completely controlled by the first reaction. We next investigate whether these principles are conserved in metabolic networks with more complex topologies.

Branch point with two upstream fluxes

We next consider a metabolic network with two converging fluxes, J_1 and J_2, at a branch point (Fig. 3*A*). Through the two fluxes, the metabolite at the branch point, S_{BP}, is produced by two input substrates, $S_{in,1}$ and $S_{in,2}$. The final product S_{out} is produced from S_{BP} with the flux $J_1 + J_2$ at the steady state. The three reactions included in this network have rate constants $\{k_1, k_2, k_3\}$ and equilibrium constants $\{K_1, K_2, K_3\}$. At the steady state, the fluxes J_1 and J_2 and the concentration of S_{BP} can be solved from the rate constants, equilibrium constants, and concentrations of the input substrates and end product based on the kinetic rules.

$$\begin{cases} J_1 = k_1(S_{in,1} - \dfrac{S_{BP}}{K_1}) \\ J_2 = k_2(S_{in,2} - \dfrac{S_{BP}}{K_2}) \\ J_1 + J_2 = k_3(S_{BP} - \dfrac{S_{out}}{K_3}) \end{cases} \quad \text{(Eq. 3.1)}$$

From Equation 3.1, we can solve the steady-state concentration of the branch point metabolite, S_{BP},

$$S_{BP} = \frac{k_1 S_{in,1} + k_2 S_{in,2} + \dfrac{k_3}{K_3} S_{out}}{\dfrac{k_1}{K_1} + \dfrac{k_2}{K_2} + k_3} \quad \text{(Eq. 3.2)}$$

and the steady-state fluxes,

$$\begin{cases} J_1 = k_1\left(S_{in,1} - \dfrac{K_2(k_1K_3S_{in,1} + k_2K_3S_{in,2} + k_3S_{out})}{(k_1K_2 + K_1k_2 + K_1K_2k_3)K_3}\right) \\ J_2 = k_2\left(S_{in,2} - \dfrac{K_1(k_1K_3S_{in,1} + k_2K_3S_{in,2} + k_3S_{out})}{(k_1K_2 + K_1k_2 + K_1K_2k_3)K_3}\right) \end{cases} \quad \text{(Eq. 3.3)}$$

We can then determine the flux control coefficients from the summation and the connectivity theorems. Here, we have three fluxes and three reactions in the network, giving nine flux control coefficients.

$$\mathbf{C}^{\mathbf{J}}_{\mathbf{v}} = \begin{pmatrix} \dfrac{\partial \log J_1}{\partial \log k_1} & \dfrac{\partial \log J_1}{\partial \log k_2} & \dfrac{\partial \log J_1}{\partial \log k_3} \\ \dfrac{\partial \log J_2}{\partial \log k_1} & \dfrac{\partial \log J_2}{\partial \log k_2} & \dfrac{\partial \log J_2}{\partial \log k_3} \\ \dfrac{\partial \log (J_1 + J_2)}{\partial \log k_1} & \dfrac{\partial \log (J_1 + J_2)}{\partial \log k_2} & \dfrac{\partial \log (J_1 + J_2)}{\partial \log k_3} \end{pmatrix} \quad \text{(Eq. 3.4)}$$

These flux control coefficients can be determined based on the summation theorem and connectivity theorem,

Summation theorem

$$\mathbf{C}^{\mathbf{J}}_{\mathbf{v}} \begin{pmatrix} \dfrac{1}{J_1} & 0 & 0 \\ 0 & \dfrac{1}{J_2} & 0 \\ 0 & 0 & \dfrac{1}{J_1 + J_2} \end{pmatrix} \mathbf{K} = \begin{pmatrix} \dfrac{1}{J_1} & 0 & 0 \\ 0 & \dfrac{1}{J_2} & 0 \\ 0 & 0 & \dfrac{1}{J_1 + J_2} \end{pmatrix} \mathbf{K} \quad \text{(Eq. 3.5)}$$

in which columns of **K** are the linear basis of feasible steady-state flux configurations in the network (*i.e.* all feasible steady-

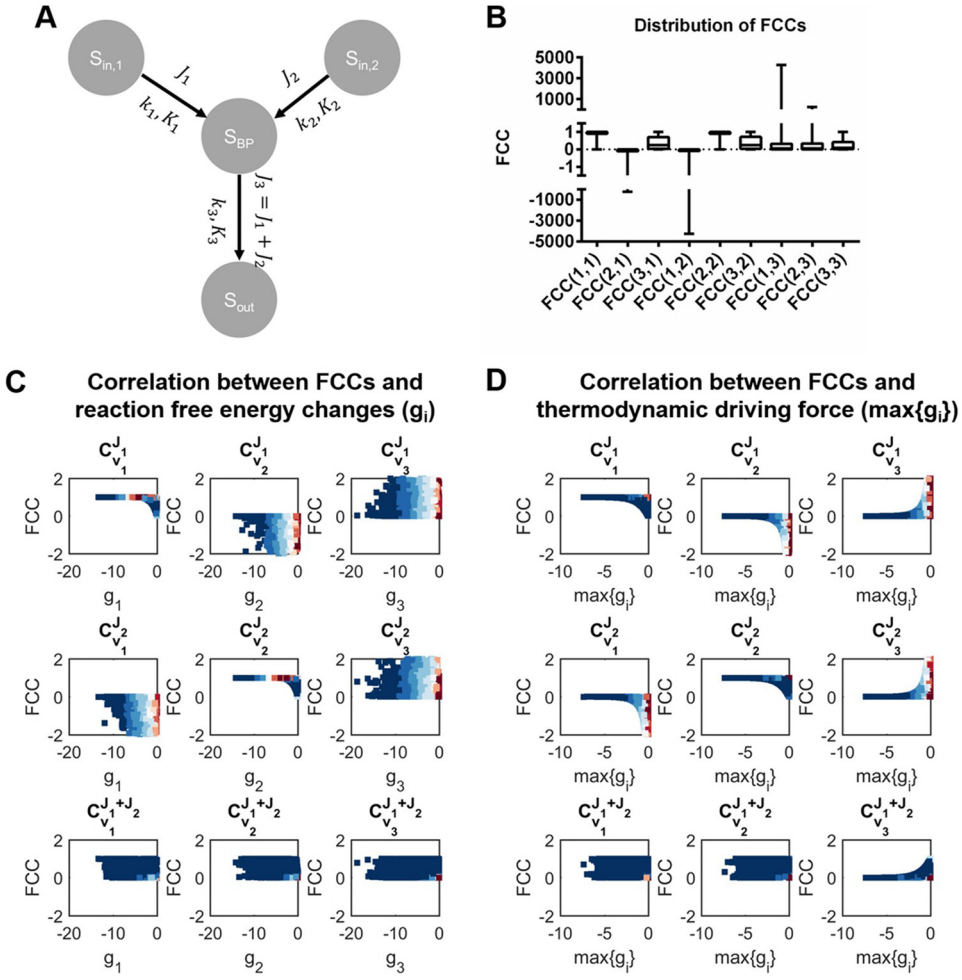

Figure 3. Thermodynamics and flux regulation in a pathway with a branch point and two upstream fluxes. *A*, diagram of the pathway and related parameters. $S_{in,1}$ and $S_{in,2}$ are the two input substrates, S_{out} is the final product, S_{BP} is the intermediary metabolite at branch point, k_i is the rate constant of the *i*th reaction, K_i is the equilibrium constant of the *i*th reaction, J_1 and J_2 are two upstream fluxes, and $J_3 = J_1 + J_2$ is the downstream flux. *B*, distributions of the flux control coefficients for the network in *A* with randomly sampled parameters. FCC(i,j) = C_{vi}^{Jj} is the flux control coefficient of the *i*th flux with respect to the *j*th reaction. *Limits* of the *boxes* are the 25th and 75th percentiles, *central lines* are median values, and *whiskers* indicate minimal and maximal values. *C*, scatter plots comparing flux control coefficients and reaction free energy changes in the network in *A* with randomly sampled parameters. $C_{v_i}^{J_i}$ is the *i*th flux control coefficient, and $g_i = \Delta G_i/RT$ quantifies the *i*th free energy change. *D*, scatter plots comparing flux control coefficients and the thermodynamic driving force (max{g_i}) in the network in *A* with randomly sampled parameters. Variables are the same as in *C*.

state flux configurations can be written in the form of linear combination of columns of **K**).

$$\mathbf{K} = \begin{pmatrix} 1 & 0 \\ 0 & 1 \\ 1 & 1 \end{pmatrix} \qquad \text{(Eq. 3.6)}$$

It is worth noting that Equation 3.5 is not sufficient for determining all values of the flux control coefficients because it provides six linear equations for nine unknowns. To uniquely calculate every element of C_v^J, three additional equations from the connectivity theorem are needed.

Connectivity theorem

$$\mathbf{C}_v^J \boldsymbol{\epsilon} = \mathbf{0} \qquad \text{(Eq. 3.7)}$$

In Equation 3.7, $\boldsymbol{\epsilon}$ represents the matrix consisting of the normalized elasticity coefficients.

$$\boldsymbol{\varepsilon} = \begin{pmatrix} \frac{S_{BP}}{v_1}\frac{\partial v_1}{\partial S_{BP}} \\ \frac{S_{BP}}{v_2}\frac{\partial v_2}{\partial S_{BP}} \\ \frac{S_{BP}}{v_3}\frac{\partial v_3}{\partial S_{BP}} \end{pmatrix} = \begin{pmatrix} \frac{S_{BP}}{S_{BP} - K_1 S_{in,1}} \\ \frac{S_{BP}}{S_{BP} - K_2 S_{in,2}} \\ \frac{K_3 S_{BP}}{K_3 S_{BP} - S_{out}} \end{pmatrix} = \begin{pmatrix} \frac{1}{1 - e^{-g_1}} \\ \frac{1}{1 - e^{-g_2}} \\ \frac{1}{1 - e^{g_3}} \end{pmatrix} \qquad \text{(Eq. 3.8)}$$

Thus, by combining Equations 3.1–3.8, the flux control coefficients can be uniquely solved.

$$\begin{cases} C_{v_1}^{J_1} = \dfrac{K_1(k_2+K_2k_3)}{k_1K_2+K_1(k_2+K_2k_3)} \\ C_{v_1}^{J_2} = \dfrac{k_1K_1(K_1(k_2+K_2k_3)K_3S_{in,1}-K_2(k_2K_3S_{in,2}+k_3S_{out}))}{(k_1K_2+K_1(k_2+K_2k_3))(k_1K_3(K_1S_{in,1}-K_2S_{in,2})+K_1k_3(S_{out}-K_2K_3S_{in,2}))} \\ C_{v_1}^{J_1+J_2} = \dfrac{k_1K_1K_2(K_1(k_2+K_2k_3)K_3S_{in,1}-K_2(k_2K_3S_{in,2}+k_3S_{out}))}{(k_1K_2+K_1(k_2+K_2k_3))(k_1K_2(K_1K_3S_{in,1}-S_{out})+K_1k_2(K_2K_3S_{in,2}-S_{out}))} \\ C_{v_2}^{J_1} = -\dfrac{k_2K_2(-k_1K_1K_3S_{in,1}+k_1K_2K_3S_{in,2}+K_1K_2k_3K_3S_{in,2}-K_1k_3S_{out})}{(k_1K_2+K_1(k_2+K_2k_3))(K_1(k_2+K_2k_3)K_3S_{in,1}-K_2(k_2K_3S_{in,2}+k_3S_{out}))} \\ C_{v_2}^{J_2} = \dfrac{K_2(k_1+K_1k_3)}{k_1K_2+K_1(k_2+K_2k_3)} \\ C_{v_2}^{J_1+J_2} = \dfrac{K_1k_2K_2(-k_1K_1K_3S_{in,1}+k_1K_2K_3S_{in,2}+K_1K_2k_3K_3S_{in,2}-K_1k_3S_{out})}{(k_1K_2+K_1(k_2+K_2k_3))(k_1K_2(K_1K_3S_{in,1}-S_{out})+K_1k_2(K_2K_3S_{in,2}-S_{out}))} \\ C_{v_3}^{J_1} = \dfrac{K_2k_3(k_1K_2(K_1K_3S_{in,1}-S_{out})+K_1k_2(K_2K_3S_{in,2}-S_{out}))}{(k_1K_2+K_1(k_2+K_2k_3))(K_1(k_2+K_2k_3)K_3S_{in,1}-K_2(k_2K_3S_{in,2}+k_3S_{out}))} \\ C_{v_3}^{J_2} = \dfrac{K_1k_3(k_1K_2(K_1K_3S_{in,1}-S_{out})+K_1k_2(K_2K_3S_{in,2}-S_{out}))}{(k_1K_2+K_1(k_2+K_2k_3))(-k_1K_1K_3S_{in,1}+k_1K_2K_3S_{in,2}+K_1K_2k_3K_3S_{in,2}-K_1k_3S_{out})} \\ C_{v_3}^{J_1+J_2} = \dfrac{K_1k_2+k_1K_2}{K_1k_2+k_1K_2+K_1K_2k_3} \end{cases} \quad \text{(Eq. 3.9)}$$

Furthermore, the reaction free energy changes can also be written as functions of the kinetic parameters and substrate concentrations.

$$\begin{cases} e^{g_1} = \dfrac{k_1K_2K_3S_{in,1}+k_2K_2K_3S_{in,2}+K_2k_3S_{out}}{K_1k_2K_3S_{in,1}+k_1K_2K_3S_{in,1}+K_1K_2k_3K_3S_{in,1}} \\ e^{g_2} = \dfrac{k_1K_1K_3S_{in,1}+K_1k_2K_3S_{in,2}+K_1k_3S_{out}}{K_1k_2K_3S_{in,2}+k_1K_2K_3S_{in,2}+K_1K_2k_3K_3S_{in,2}} \\ e^{g_3} = \dfrac{K_1k_2S_{out}+k_1K_2S_{out}+K_1K_2k_3S_{out}}{k_1K_1K_2K_3S_{in,1}+K_1k_2K_2K_3S_{in,2}+K_1K_2k_3S_{out}} \end{cases} \quad \text{(Eq. 3.10)}$$

We then combine Equations 3.9 and 3.10 to express the flux control coefficients in terms of the reaction parameters and free energy terms. To simplify the expressions, we let $h_i = e^{gi}$. Then we have the following.

$$\begin{cases} C_{v_1}^{J_1} = \dfrac{K_1(k_2+K_2k_3)}{k_1K_2+K_1(k_2+K_2k_3)} \\ C_{v_1}^{J_2} = -\dfrac{(h_1-1)h_2k_1K_2}{h_1(h_2-1)(k_1K_2+K_1k_2+K_1K_2k_3)} \\ C_{v_1}^{J_1+J_2} = \dfrac{(h_1-1)h_2k_1K_1K_2{}^2k_3}{(h_1(h_2-1)K_1k_2+(h_1-1)h_2k_1K_2)(k_1K_2+K_1k_2+K_1K_2k_3)} \\ C_{v_2}^{J_1} = -\dfrac{h_1(h_2-1)K_1k_2}{(h_1-1)h_2(k_1K_2+K_1k_2+K_1K_2k_3)} \\ C_{v_2}^{J_2} = \dfrac{K_2(k_1+K_1k_3)}{k_1K_2+K_1(k_2+K_2k_3)} \\ C_{v_2}^{J_1+J_2} = \dfrac{h_1(h_2-1)K_1{}^2k_2K_2k_3}{(h_1(h_2-1)K_1k_2+(h_1-1)h_2k_1K_2)(k_1K_2+K_1k_2+K_1K_2k_3)} \\ C_{v_3}^{J_1} = \dfrac{(h_1(h_2-1)K_1k_2+(h_1-1)h_2k_1K_2)}{(h_1-1)h_2(k_1K_2+K_1k_2+K_1K_2k_3)} \\ C_{v_3}^{J_2} = \dfrac{(h_1(h_2-1)K_1k_2+(h_1-1)h_2k_1K_2)}{h_1(h_2-1)(k_1K_2+K_1k_2+K_1K_2k_3)} \\ C_{v_3}^{J_1+J_2} = \dfrac{K_1k_2+k_1K_2}{K_1k_2+k_1K_2+K_1K_2k_3} \end{cases} \quad \text{(Eq. 3.11)}$$

To illustrate the relationships between flux control coefficients and thermodynamic properties of the network, according to Equations 3.9–3.11, we simulate the flux control coefficients and reaction free energy changes based on 20,000 combinations of parameters randomly sampled from a log-normal distribution as described previously in Equation 2.9. Combinations of parameters resulting in negative fluxes are discarded. The distributions of flux control coefficients (Fig. 3*B*) show that C_{v2}^{J1}, C_{v1}^{J2}, C_{v3}^{J1}, and C_{v3}^{J2} can have absolute values much larger than 1 under certain parameter combinations, indicating that the two upstream fluxes can be dramatically altered in response to perturbation of activities of enzymes in other branches. Based on the simulation, we also compare flux control coefficients with the reaction free energy changes (Fig. 3*C*) and the thermodynamic driving force (Fig. 3*D*). Consistent with the case of the linear pathway, most of the flux control coefficients correlate poorly with free energy changes of the individual reactions catalyzed by the corresponding enzyme (Fig. 3*C*) but exhibit a dependence on the thermodynamic driving force (Fig. 3*D*). Moreover, the quantitative relationships characterizing how flux control coefficients are constrained by the thermodynamic driving force can also be analytically derived (see the supporting information).

$$\begin{cases} C_{v_1}^{J_1} > 1-e^{TDF} \\ C_{v_2}^{J_1} > -\dfrac{e^{TDF}}{1-e^{TDF}} \\ C_{v_3}^{J_1} < \dfrac{e^{TDF}}{1-e^{TDF}} \\ C_{v_1}^{J_2} > -\dfrac{e^{TDF}}{1-e^{TDF}} \\ C_{v_2}^{J_2} > 1-e^{TDF} \\ C_{v_3}^{J_2} < \dfrac{e^{TDF}}{1-e^{TDF}} \\ C_{v_3}^{J_1+J_2} < e^{TDF} \end{cases} \quad \text{(Eq. 3.12)}$$

From Equation 3.12, we can derive the limits of all the flux control coefficients except for C_{v1}^{J1+J2} and C_{v2}^{J1+J2} when the thermodynamic driving force goes to minus infinity.

$$\begin{cases} \lim\limits_{TDF\to-\infty} C_{v_1}^{J_1} = 1 \\ \lim\limits_{TDF\to-\infty} C_{v_2}^{J_1} = 0 \\ \lim\limits_{TDF\to-\infty} C_{v_3}^{J_1} = 0 \\ \lim\limits_{TDF\to-\infty} C_{v_1}^{J_2} = 0 \\ \lim\limits_{TDF\to-\infty} C_{v_2}^{J_2} = 1 \\ \lim\limits_{TDF\to-\infty} C_{v_3}^{J_2} = 0 \\ \lim\limits_{TDF\to-\infty} C_{v_3}^{J_1+J_2} = 0 \end{cases} \quad \text{(Eq. 3.13)}$$

Thus, when the pathway is far from equilibrium, the two upstream fluxes J_1 and J_2 are fully regulated by activities of the

enzymes that generate them. Moreover, the downstream flux $J_1 + J_2$ is also fully controlled by the two upstream enzymes. The inequalities in Equation 3.12 also indicate that the feasible regions of the flux control coefficients C_{v2}^{J1}, C_{v1}^{J2}, C_{v3}^{J1}, and C_{v3}^{J2} become semi-infinite (*i.e.* only bounded in one direction) when the thermodynamic driving force approaches zero (*i.e.* there exists at least one near-equilibrium reaction in this pathway).

To summarize, in a metabolic pathway with a branch point involving two converging fluxes, regulation of the fluxes is largely dependent on how close to thermodynamic equilibrium the pathway in entirety is. When the pathway is far away from equilibrium, all three fluxes are completely controlled by the two upstream enzymes. On the other hand, when there exists at least one near-equilibrium reaction in the pathway, there is more flexibility in the regulation of fluxes, and, unlike in the case of linear pathways, the two upstream fluxes are able to be dramatically altered even by enzymes that are not directly involved in the reaction.

Branch point with two downstream fluxes

We next consider a pathway with one branch point in which one upstream flux, J_1, diverges to two downstream fluxes, J_2 and J_3, and show that the principles of metabolic flux regulation and thermodynamics also hold in this case. This network includes one input substrate, S_{in}, and two final products, $S_{out,1}$ and $S_{out,2}$, which are all connected to the branch point metabolite S_{BP}. All kinetic rules and assumptions are as described above. Thus, at the steady state, concentration of S_{BP} can be solved from the reaction parameters and concentrations of other metabolites in the network.

$$S_{BP} = \frac{k_1 S_{in} + \frac{k_2}{K_2} S_{out,1} + \frac{k_3}{K_3} S_{out,2}}{\frac{k_1}{K_1} + k_2 + k_3} \quad \text{(Eq. 4.1)}$$

Fluxes and reaction free energy changes at the steady state can also be calculated from Equation 4.1.

$$\begin{cases} J_2 = k_2 \left(\dfrac{k_1 S_{in} + \frac{k_2}{K_2} S_{out,1} + \frac{k_3}{K_3} S_{out,2}}{\frac{k_1}{K_1} + k_2 + k_3} - \dfrac{S_{out,1}}{K_2} \right) \\ J_3 = k_3 \left(\dfrac{k_1 S_{in} + \frac{k_2}{K_2} S_{out,1} + \frac{k_3}{K_3} S_{out,2}}{\frac{k_1}{K_1} + k_2 + k_3} - \dfrac{S_{out,2}}{K_3} \right) \end{cases} \quad \text{(Eq. 4.2)}$$

$$\begin{cases} e^{g_1} = \dfrac{k_1 K_2 K_3 S_{in} + k_2 K_3 S_{out,1} + K_2 k_3 S_{out,2}}{(k_1 + K_1 k_2 + K_1 k_3) K_2 K_3 S_{in}} \\ e^{g_2} = \dfrac{(k_1 + K_1 k_2 + K_1 k_3) K_3 S_{out,1}}{K_1 (k_1 K_2 K_3 S_{in} + k_2 K_3 S_{out,1} + K_2 k_3 S_{out,2})} \\ e^{g_3} = \dfrac{(k_1 + K_1 k_2 + K_1 k_3) K_2 S_{out,2}}{K_1 (k_1 K_2 K_3 S_{in} + k_2 K_3 S_{out,1} + K_2 k_3 S_{out,2})} \end{cases} \quad \text{(Eq. 4.3)}$$

Here, we also have in total nine flux control coefficients that can be solved based on the summation theorem and connectivity theorem.

$$\mathbf{C}_{\mathrm{v}}^{\mathbf{J}} = \begin{pmatrix} \frac{\partial \log(J_2 + J_3)}{\partial \log k_1} & \frac{\partial \log(J_2 + J_3)}{\partial \log k_2} & \frac{\partial \log(J_2 + J_3)}{\partial \log k_3} \\ \frac{\partial \log J_2}{\partial \log k_1} & \frac{\partial \log J_2}{\partial \log k_2} & \frac{\partial \log J_2}{\partial \log k_3} \\ \frac{\partial \log J_3}{\partial \log k_1} & \frac{\partial \log J_3}{\partial \log k_2} & \frac{\partial \log J_3}{\partial \log k_3} \end{pmatrix} \quad \text{(Eq. 4.4)}$$

$$\mathbf{C}_{\mathrm{v}}^{\mathbf{J}} \begin{pmatrix} \frac{1}{J_2 + J_3} & \frac{1}{J_2 + J_3} & \frac{S_{BP}}{S_{BP} - K_1 S_{in}} \\ \frac{1}{J_2} & 0 & \frac{K_2 S_{BP}}{K_2 S_{BP} - S_{out,1}} \\ 0 & \frac{1}{J_3} & \frac{K_3 S_{BP}}{K_3 S_{BP} - S_{out,2}} \end{pmatrix} = \begin{pmatrix} \frac{1}{J_2 + J_3} & \frac{1}{J_2 + J_3} & 0 \\ \frac{1}{J_2} & 0 & 0 \\ 0 & \frac{1}{J_3} & 0 \end{pmatrix} \quad \text{(Eq. 4.5)}$$

By combining Equations 4.2–4.5, we can also determine the flux control coefficients as functions of reaction parameters and free energy changes.

$$\begin{cases} C_{v_1}^{J_2+J_3} = \dfrac{K_1(k_2 + k_3)}{k_1 + K_1(k_2 + k_3)} \\ C_{v_1}^{J_2} = \dfrac{K_1((h_2 - 1)k_2 + (h_3 - 1)k_3)}{(h_2 - 1)(k_1 + K_1(k_2 + k_3))} \\ C_{v_1}^{J_3} = \dfrac{K_1((h_2 - 1)k_2 + (h_3 - 1)k_3)}{(h_3 - 1)(k_1 + K_1(k_2 + k_3))} \\ C_{v_2}^{J_2+J_3} = \dfrac{(h_2 - 1)k_1 k_2}{((h_2 - 1)k_2 + (h_3 - 1)k_3)(k_1 + K_1(k_2 + k_3))} \\ C_{v_2}^{J_2} = \dfrac{k_1 + K_1 k_3}{k_1 + K_1(k_2 + k_3)} \\ C_{v_2}^{J_3} = -\dfrac{(h_2 - 1)K_1 k_2}{(h_3 - 1)(k_1 + K_1(k_2 + k_3))} \\ C_{v_3}^{J_2+J_3} = \dfrac{(h_3 - 1)k_1 k_3}{((h_2 - 1)k_2 + (h_3 - 1)k_3)(k_1 + K_1(k_2 + k_3))} \\ C_{v_3}^{J_2} = -\dfrac{(h_3 - 1)K_1 k_3}{(h_2 - 1)(k_1 + K_1(k_2 + k_3))} \\ C_{v_3}^{J_3} = \dfrac{k_1 + K_1 k_2}{k_1 + K_1(k_2 + k_3)} \end{cases} \quad \text{(Eq. 4.6)}$$

To investigate the relationships between flux control coefficients and thermodynamic variables, we randomly sample 20,000 combinations of reaction parameters and substrate concentrations and calculate flux control coefficients and free energy changes corresponding to the randomly sampled parameters from Equations 4.3 and 4.6. Distributions of the sampled flux control coefficients suggest that the two downstream fluxes are able to be regulated in response to variations in the activity of enzymes not directly carrying them (*i.e.* C_{v1}^{J2}, C_{v3}^{J2}, C_{v1}^{J3}, and C_{v2}^{J3}

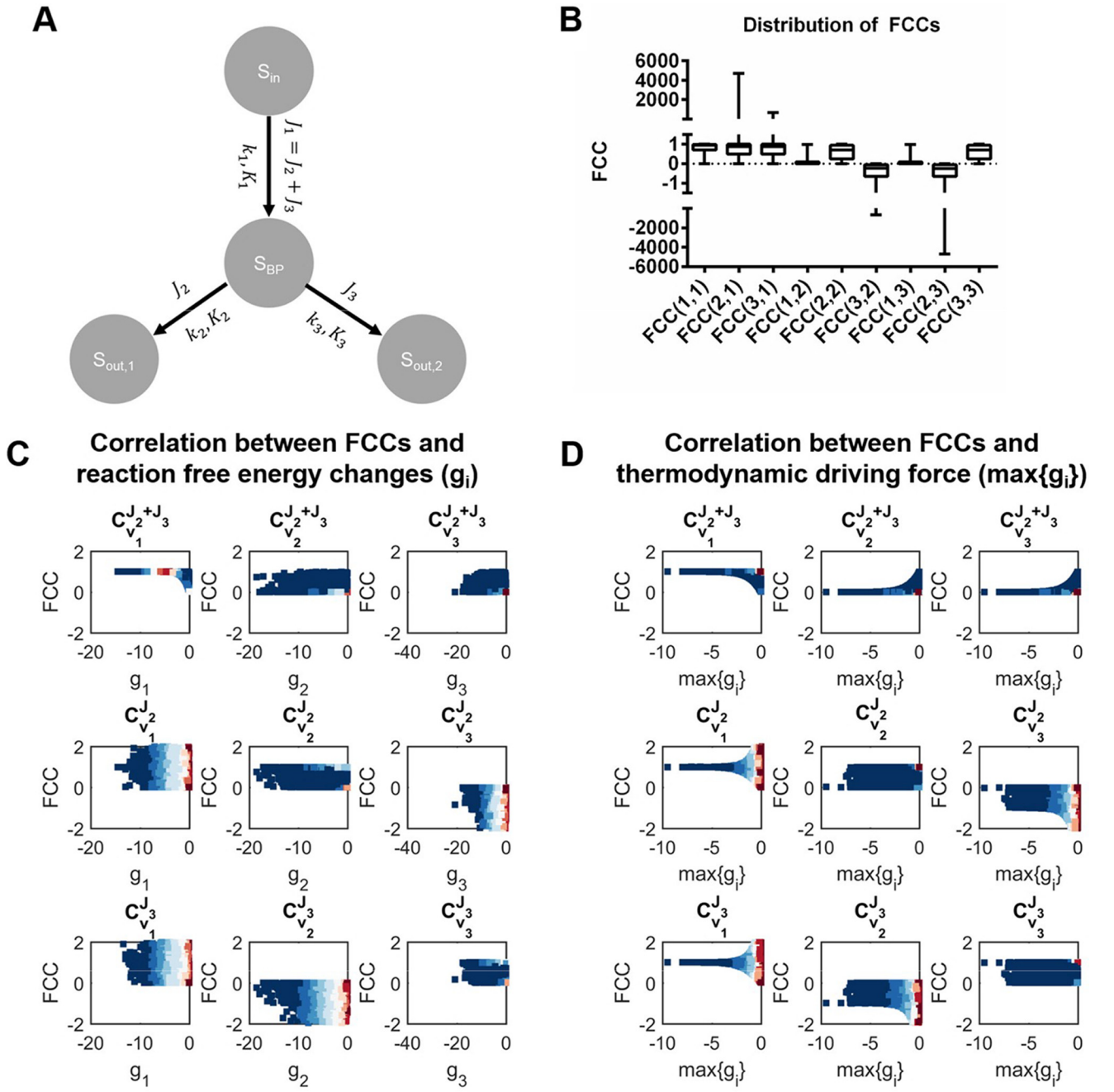

Figure 4. Thermodynamics and flux regulation in a pathway with a branch point and two downstream fluxes. *A*, diagram of the pathway and related parameters. S_{in} is the input substrate, $S_{out,1}$ and $S_{out,2}$ are the two final products, S_{BP} is the intermediary metabolite at branch point, k_i is the rate constant of the *i*th reaction, K_i is the equilibrium constant of the *i*th reaction, J_2 and J_3 are two downstream fluxes, and $J_1 = J_2 + J_3$ is the upstream flux. *B*, distribution of the flux control coefficients for the network in *A* with randomly sampled parameters. FCC(*i*,*j*) = $C_{vj}^{J_i}$ is the flux control coefficient of the *i*th flux with respect to the *j*th reaction. *Limits* of the *boxes* are the 25th and 75th percentiles, *central lines* are median values, and *whiskers* indicate minimal and maximal values. *C*, scatter plots comparing flux control coefficients and reaction free energy changes in the network in *A* with randomly sampled parameters. $C_{vi}^{J_i}$ is the *i*th flux control coefficient, and $g_i = \Delta G_i/RT$ quantifies the *i*th free energy change. *D*, scatter plots comparing flux control coefficients and the thermodynamic driving force (max{g_i}) in the network in *A* with randomly sampled parameters. Variables are the same as in *C*.

can have absolute values larger than 1; Fig. 4*B*). Again, we observe a poor correlation between flux control coefficients and free energy change of the corresponding reaction steps (Fig. 4*C*). Among the nine flux control coefficients, only C_{v1}^{J2+J3} exhibits a clear dependence on the free energy change g_1.

Despite the poor correlation between flux control coefficients and free energy changes of individual reaction steps, seven of the nine flux control coefficients are strictly constrained by the thermodynamic driving force (Fig. 4*D*). This corroborates the findings in other types of network topologies that the regulation of metabolic fluxes is constrained by the deviation of the whole pathway from thermodynamic equilibrium. We also analytically derive the quantitative relationships between the upper and lower bounds of the flux control coefficients and the thermodynamic driving force of the pathway (see the supporting information).

$$\begin{cases} C_{v_1}^{J_2+J_3} > 1-e^{TDF} \\ C_{v_2}^{J_2+J_3} < e^{TDF} \\ C_{v_3}^{J_2+J_3} < e^{TDF} \\ C_{v_1}^{J_2} > \left(1-e^{TDF}\right)^2 \\ C_{v_1}^{J_2} < \dfrac{1}{1-e^{TDF}} \\ C_{v_3}^{J_2} > -\dfrac{1}{1-e^{TDF}} \\ C_{v_1}^{J_3} > \left(1-e^{TDF}\right)^2 \\ C_{v_1}^{J_3} < \dfrac{1}{1-e^{TDF}} \\ C_{v_2}^{J_3} > -\dfrac{1}{1-e^{TDF}} \end{cases} \quad \text{(Eq. 4.7)}$$

According to Equation 4.7, when the network moves away from the thermodynamic equilibrium, many of the flux control coefficients converge to fixed values.

$$\begin{cases} \lim\limits_{TDF\to-\infty} C_{v_1}^{J_2+J_3} = 1 \\ \lim\limits_{TDF\to-\infty} C_{v_2}^{J_2+J_3} = 0 \\ \lim\limits_{TDF\to-\infty} C_{v_3}^{J_2+J_3} = 0 \\ \lim\limits_{TDF\to-\infty} C_{v_1}^{J_2} = 1 \\ \lim\limits_{TDF\to-\infty} C_{v_1}^{J_3} = 1 \end{cases} \quad \text{(Eq. 4.8)}$$

Thus, when the pathway is far away from thermodynamic equilibrium, the enzyme catalyzing the upstream reaction exerts complete control of all three fluxes. Larger variability in all flux control coefficients that result in semi-infinite feasible regions of the flux control coefficients C_{v1}^{J2}, C_{v3}^{J2}, C_{v1}^{J3}, and C_{v2}^{J3} are allowed only when there exist near-equilibrium reactions in this network.

Thus, based on a combination of analysis and simulation, we have demonstrated that, at branch points, the regulation of fluxes by enzyme activities is constrained by the thermodynamic driving force but has little correlation with free energy changes of the individual enzymes. These findings, together with similar results in other network structures, suggest that the influences of thermodynamics on regulation of metabolic fluxes by enzyme activities primarily occur at the pathway level rather than at the individual reaction level. These principles are applicable to simple metabolic network models regardless of the structure of the metabolic network, but they also rely on the assumption that all enzymes follow first-order kinetics. We next examine whether the conclusions are conserved in metabolic networks with Michaelis–Menten kinetics.

Thermodynamics and flux control in Michaelis–Menten models

We now consider zero-order kinetic models as an extreme case of substrate-saturable enzymes and repeat the theoretical analysis and simulation in these models to characterize the relationships between thermodynamics and flux control. Briefly, although the expressions of steady-state concentrations of the intermediary metabolites and steady-state fluxes are much more complicated with this assumption, the flux control coefficients can still be written in the form of simple functions of the reaction parameters and free energy changes. However, the thermodynamic driving force no longer constrains the flux control coefficients in this case (Figs. S1 and S2). Most of the flux control coefficients in all three network structures have the form of a zero-order homogeneous function of the thermodynamic terms h_i. Consequently, moving all reactions away from or toward the thermodynamic equilibrium without influencing the ratios between the h_i values does not change the resulting flux control coefficients.

Because flux control is no longer constrained by the thermodynamic driving force in zero-order kinetic models, we hypothesize that in Michaelis–Menten models, which lie between the extreme cases of first-order and zero-order kinetic models, the saturation of enzymes by metabolites determines whether the flux control coefficients are still constrained by the thermodynamic driving force as they are in first-order kinetic models. In Michaelis–Menten models (28), the rate of a reaction depends on the catalytic constant (*i.e.* turnover number) k and the equilibrium constant K of the enzyme, the concentrations of its substrate S and product P, and the Michaelis–Menten constants K_S and K_P for the substrate and product, respectively.

$$v = k\left(\frac{\frac{S}{K_S}}{1+\frac{S}{K_S}+\frac{P}{K_P}}\right)\left(1-\frac{P}{KS}\right) \quad \text{(Eq. 5.1)}$$

We note that for Michaelis–Menten models, the elasticity coefficients toward the substrate and product concentrations differ from those in first-order kinetic models only by one term quantifying saturation of the enzyme by the given metabolite (*i.e.* substrate or product).

$$\begin{cases} \varepsilon_S = \dfrac{1}{1-e^{g}} - \dfrac{S/K_S}{1+S/K_S+P/K_P} \\ \varepsilon_P = \dfrac{1}{1-e^{-g}} - \dfrac{P/K_P}{1+S/K_S+P/K_P} \end{cases} \quad \text{(Eq. 5.2)}$$

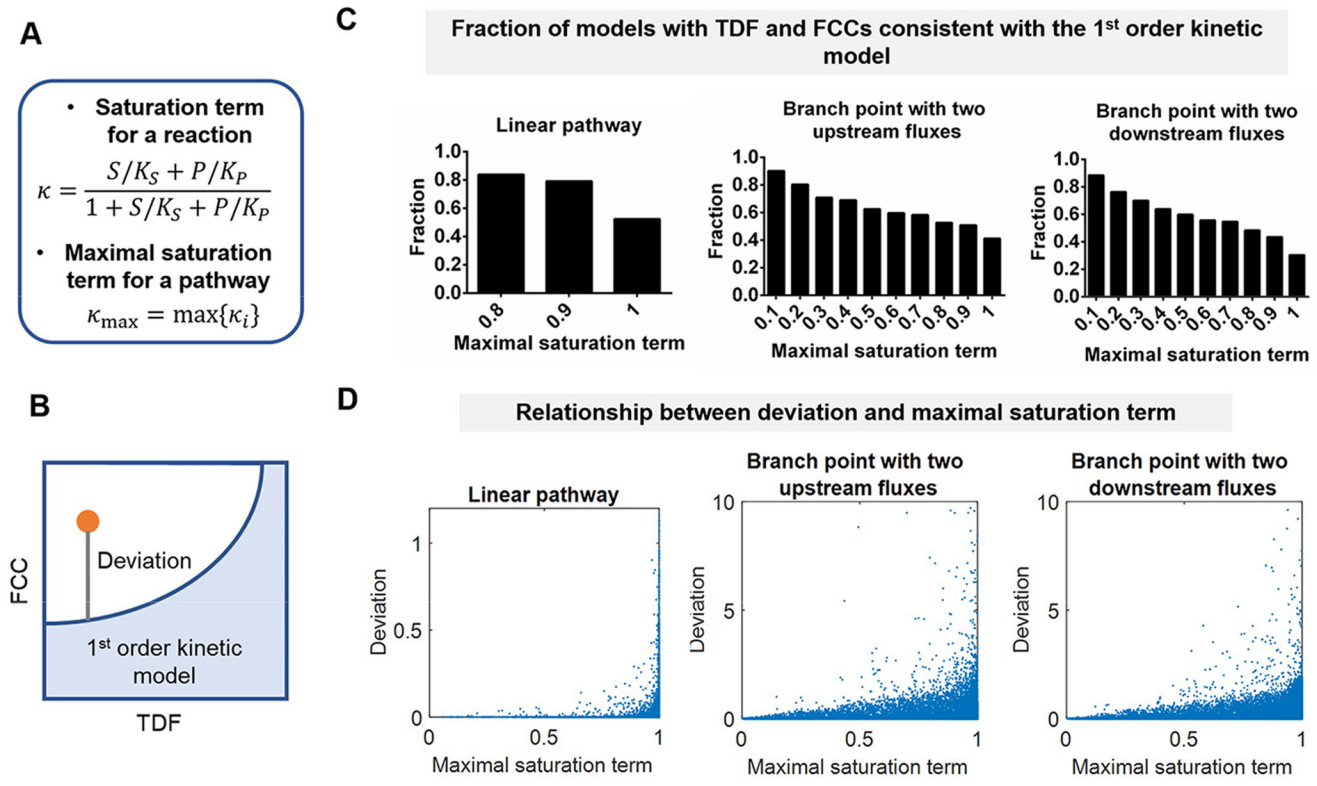

Figure 5. Thermodynamics and flux control in Michaelis–Menten models. *A*, definition of saturation term for a reaction and maximal saturation term for a metabolic pathway. *B*, deviation of FCCs and TDF in a Michaelis–Menten model (*orange dot*) from relationships derived in the first-order kinetic model (*light blue shaded region*). *C*, relationship between maximal saturation term and fraction of Michaelis–Menten models with TDF and FCCs consistent with the first-order kinetic model. *D*, relationship between deviation from first-order kinetic model and maximal saturation term in Michaelis–Menten models.

For Michaelis–Menten models, because the rate law is more complicated than that of zero-order or first-order kinetic models, we use sets of parameters randomly generated, as previously done for first-order kinetic models to simulate the thermodynamic variables and flux control coefficients, and then compare them with those in first-order kinetic models. To quantify the saturation of enzymes, we introduce the saturation term for a reaction (Fig. 5*A*). This saturation term considers the total saturation of an enzyme by the substrate and the product.

$$\kappa = \frac{\frac{S}{K_S} + \frac{P}{K_P}}{1 + \frac{S}{K_S} + \frac{P}{K_P}} \qquad \text{(Eq. 5.3)}$$

For a pathway, the overall level of enzyme saturation is quantified by the maximal saturation term (Fig. 5*A*).

$$\kappa_{max} = \max\{\kappa_i\} \qquad \text{(Eq. 5.4)}$$

To evaluate whether the thermodynamic variables and flux control coefficients in a Michaelis–Menten model are consistent with the relationships we have derived for first-order kinetic models, we compute the deviation of the flux control coefficients in the Michaelis–Menten model from those allowed in the first-order kinetic model with the same topology and thermodynamic driving force (Fig. 5*B*).

We first examine how the maximal saturation term affects the fraction of Michaelis–Menten models consistent with first-order kinetic models. In all three pathway structures, we observe a gradual increase in the fraction of Michaelis–Menten models consistent with the first-order kinetic models (Fig. 5*C*) as the maximal saturation term decreases, suggesting that the flux control coefficients are largely constrained by the thermodynamic driving force when the enzymes in the pathway are not highly saturated. We next compare the maximal saturation term with the deviation from the results in the first-order kinetic model. We find that the deviation gradually decreases as the maximal saturation term decreases, corroborating the findings that the relationships between thermodynamics and flux control are conserved in Michaelis–Menten models if the enzymes are not highly saturated.

To summarize, here we show that the principles for thermodynamics and flux control in metabolic pathways with first-order kinetics are still effective in Michaelis–Menten models if the enzymes are not highly saturated. It is now reasonable to ask whether the same rules apply to more complicated metabolic networks in which most enzymes not only follow the Michaelis–Menten kinetics, but also have their activities regulated by long-range interactions such as allosteric feedback.

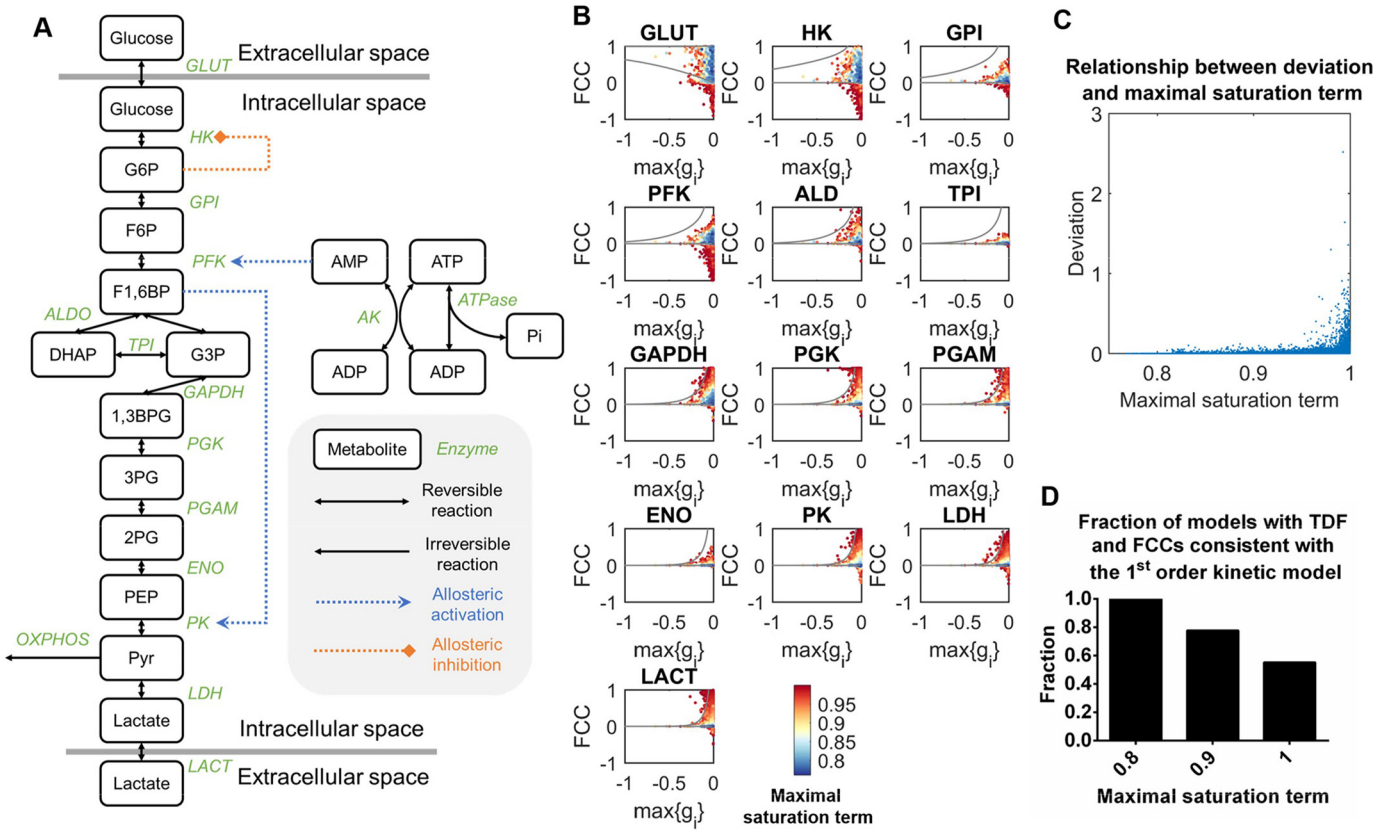

Figure 6. Thermodynamics and flux control in a mathematical model of glycolysis. *A*, diagram of the glycolysis model. *B*, scatter plots comparing TDF and FCCs of the glycolytic flux (*i.e.* the rate of conversion of glucose to pyruvate) with respect to each reaction step. Each *point* represents a set of randomly generated parameters. *Color* of a *point* indicates the maximal saturation term under the corresponding set of parameters. *Gray lines*, upper and lower bounds derived under the assumption of first-order kinetics. *C*, scatter plot comparing maximal saturation term and deviation from first-order kinetics in the glycolysis model. *D*, relationship between maximal saturation term and fraction of models with FCCs and TDF consistent with the first-order kinetic model.

Thermodynamics and flux control in a mathematical model of glycolysis

Thus, we considered a model of glycolysis to study the relationships between thermodynamics and flux control (42). We have previously constructed a mathematical model of glycolysis and used this model to study the regulation of the lactate production flux (17, 19). The topological structure of this model can be approximated by a linear pathway consisting of 13 reversible reactions (Fig. 6*A*). Elements and interactions such as reactions with more than one substrate, allosteric feedbacks, conserved species (*e.g.* NAD^+/NADH, ATP/ADP/AMP), and irreversible reactions are also included.

We generated 50,000 sets of random parameters to simulate the glycolysis model and computed the flux control coefficients and thermodynamic driving force at the steady state for each set of parameters. We also computed the maximal saturation term and assessed how the saturation of enzymes influences the relationships between thermodynamics and flux control. We first compared the thermodynamic driving force and flux control coefficients in the glycolysis model with the values allowed in the model for a linear pathway with the same number of reactions (*i.e.* 13 reactions) according to Equations 2.11 and 2.12 (Fig. 6*B*). As expected, we find that for parameter sets yielding a high (*i.e.* close to 1; *red dots* in Fig. 6*B*) maximal saturation term, the glycolysis model is inconsistent with the relationships derived under the assumption of first-order kinetics. We then estimated the deviation from first-order kinetic models (Fig. 6*C*) and computed the fraction of models consistent with first-order kinetic models (Fig. 6*D*). Consistent with the Michaelis–Menten model, we found that as the deviation decreases, the fraction of consistent models increases, suggesting that the relationships derived in first-order kinetic models with simple topological structures are largely conserved in more complicated metabolic networks.

Discussion

In this study, we derive quantitative relationships between thermodynamics, enzyme activity, and regulation of metabolic fluxes. For a set of example pathways, we calculate the flux control coefficients as functions of the enzyme rate constants, reaction equilibrium constants, and Gibbs free energy. Based on numerical simulation and exact analytical results, we find that in all network topologies considered, the flux control coefficients are bounded by the thermodynamic driving force, as defined by the deviation of the entire pathway from thermodynamic equilibrium. Moreover, distinct patterns of flux regulation emerge when the thermodynamic driving force approaches two extreme values: if the thermodynamic driving force is very negative (*i.e.* all reactions are far away from equilibrium), enzymes catalyzing the upstream reactions (*i.e.* reac-

tions directly consume the input substrates) exert full control of all fluxes; on the other hand, if the thermodynamic driving force is close to zero (*i.e.* near-equilibrium reactions exist in the pathway), there is more flexibility in the pattern of flux control, and fluxes in network topologies with branch points can be dramatically altered by enzymes not directly carrying the fluxes. These findings suggest that the coupling between thermodynamics and regulation of metabolic flux occurs at the systemic level and challenges the rule of thumb that the reaction with the most negative free energy change serves as the rate-limiting step.

It is also worth noting that all analysis that we have done to derive analytical expressions here relies on the assumption of first-order kinetics. This approximates the more generalized Michaelis–Menten mechanism when the abundance of substrate is far below the K_m of the enzyme. Accordingly, in a study comparing substrate concentrations and K_m values in different cell types, among all substrate–enzyme interactions investigated, around 70% exhibited higher substrate concentration than the K_m value, thus requiring a Michaelis–Menten or substrate-saturated, zero-order kinetics (30). For Michaelis–Menten kinetics and a glycolysis model, we have shown, that the generalizations of our findings depend on the levels of substrate saturation. We also note that the tendency of an enzyme to be operating in the linear region or to be saturated by its substrate is highly dependent on the substrate used by this enzyme. For instance, kinases use ATP as the substrate whose physiological concentration is much higher than the typical K_m value of enzymes and thus are more likely to be substrate-saturated. On the other hand, other enzymes, such as chromatin-modifying enzymes, use metabolites much less abundant as substrates (43). Nevertheless, because the relationships between thermodynamics and flux control are conserved under circumstances where the enzymes are moderately saturated, we expect that our findings are applicable to more complicated biochemical processes with Michaelis–Menten kinetics.

Finally, although the network structures that we study here are much simpler than real metabolic networks, the conclusions that we derive here can still be extended to more complicated network topologies. A metabolic network without cycles can always be simplified to a set of branch points connected by linear reaction chains with varying lengths, and the enzymes in the same linear reaction chain can be treated as an entirety to calculate the flux control coefficients with respect to simultaneous change in these enzymes (44). In this case, each linear reaction chain is simplified to a single reaction step, which enables us to apply the principles we found in the simple network structures with a branch point.

To summarize, we characterize the quantitative relationship between thermodynamics and regulation of metabolic fluxes by enzymes in a metabolic network in this study. We find that the global thermodynamic property of the network (*i.e.* thermodynamic driving force) constrains almost all flux control coefficients in both linear and branched pathways. Specifically, fluxes in metabolic networks far away from thermodynamic equilibrium are almost fully controlled by enzymes catalyzing the upstream reactions (*i.e.* reactions directly consuming the input substrates). On the other hand, near-equilibrium metabolic networks allow more flexibility in the pattern of regulation. Semi-infinite feasible regions of flux control coefficients are only allowed in branched pathways with near-equilibrium reactions. These findings highlight the importance of global thermodynamic features in constraining the pattern of regulation of metabolism.

Experimental procedures

Analytical expressions of flux control coefficients were calculated using the function LinearSolve[] in Wolfram Mathematica version 11. For the computer simulations, 20,000 combinations of random parameters were generated using the function normrnd() in MATLAB R2016b for each model. Flux control coefficients and reaction free energies were then computed using the parameter sets that generate positive flux configurations. For the glycolysis model, a model file in SBML format was downloaded from the BioModels Database (https://www.ebi.ac.uk/biomodels-main/)[4] (45) and translated to C++ codes using the SBML translator module in the Systems Biology Workbench (http://sbw.sourceforge.net/)[4] (46). Simulation of the model was done with the ODE solver gsl_odeiv2_step_msbdf in the GNU Scientific Library (https://www.gnu.org/software/gsl/).[4] 50,000 random sets of parameters were generated by sampling $V_{\max}$ values of the enzymes with Latin hypercube sampling. The flux control coefficient of the glycolytic flux (defined as the rate of glucose consumption) with respect to a reaction step was estimated using the finite difference approximation,

$$C^{J}_{v_i} = \frac{\log J_{\text{glycolysis}}(1.01V_{\max,i}) - \log J_{\text{glycolysis}}\left(\frac{V_{\max,i}}{1.01}\right)}{2\log 1.01} \quad \text{(Eq. 6.1)}$$

in which $J_{\text{glycolysis}}$ is the glycolytic flux and $V_{\max,i}$ is the maximal velocity of the ith reaction. Free energy changes for the reactions were calculated from standard reaction free energies and steady-state concentrations of the metabolites. All source codes are available at the GitHub page of the Locasale laboratory (https://github.com/LocasaleLab/MCA_thermodynamics).[4]

Author contributions—Z. D. and J. W. L. conceptualization; Z. D. data curation; Z. D. software; Z. D. and J. W. L. formal analysis; Z. D. and J. W. L. supervision; Z. D. and J. W. L. validation; Z. D. and J. W. L. investigation; Z. D. visualization; Z. D. methodology; Z. D. and J. W. L. writing-original draft; Z. D. and J. W. L. project administration; Z. D. and J. W. L. writing-review and editing; J. W. L. resources; J. W. L. funding acquisition.

Acknowledgments—We thank members of the Locasale laboratory for helpful discussions. We also thank the reviewers for insightful comments and constructive suggestions that greatly improved the manuscript.

References

1. Chandel, N. S. (2015) *Navigating Metabolism*, Cold Spring Harbor Laboratory Press, Cold Spring Harbor, NY

[4] Please note that the JBC is not responsible for the long-term archiving and maintenance of this site or any other third party hosted site.

2. Nelson, D. L., and Cox, M. M. (2016) *Lehninger Principles of Biochemistry*, 7th Ed., W. H. Freeman, New York
3. Förster, J., Famili, I., Fu, P., Palsson, B. Ø., and Nielsen, J. (2003) Genome-scale reconstruction of the *Saccharomyces cerevisiae* metabolic network. *Genome Res.* **13,** 244–253 CrossRef Medline
4. Orth, J. D., Conrad, T. M., Na, J., Lerman, J. A., Nam, H., Feist, A. M., and Palsson, B. Ø. (2011) A comprehensive genome-scale reconstruction of *Escherichia coli* metabolism–2011. *Mol. Syst. Biol.* **7,** 535 Medline
5. Brunk, E., Sahoo, S., Zielinski, D. C., Altunkaya, A., Dräger, A., Mih, N., Gatto, F., Nilsson, A., Preciat Gonzalez, G. A., Aurich, M. K., Prlić, A., Sastry, A., Danielsdottir, A. D., Heinken, A., Noronha, A., *et al.* (2018) Recon3D enables a three-dimensional view of gene variation in human metabolism. *Nat. Biotechnol.* **36,** 272–281 CrossRef Medline
6. Orth, J. D., Thiele, I., and Palsson, B. Ø. (2010) What is flux balance analysis? *Nat. Biotechnol.* **28,** 245–248 CrossRef Medline
7. Jang, C., Chen, L., and Rabinowitz, J. D. (2018) Metabolomics and isotope tracing. *Cell* **173,** 822–837 CrossRef Medline
8. Liu, X., and Locasale, J. W. (2017) Metabolomics: a primer. *Trends Biochem. Sci.* **42,** 274–284 CrossRef Medline
9. Kacser, H., and Burns, J. A. (1973) The control of flux. *Symp. Soc. Exp. Biol.* **27,** 65–104 Medline
10. Heinrich, R., and Rapoport, T. A. (1974) A linear steady-state treatment of enzymatic chains: general properties, control and effector strength. *Eur. J. Biochem.* **42,** 89–95 CrossRef Medline
11. Kacser, H., and Burns, J. A. (1981) The molecular basis of dominance. *Genetics* **97,** 639–666 Medline
12. Reder, C. (1988) Metabolic control theory: a structural approach. *J. Theor. Biol.* **135,** 175–201 CrossRef Medline
13. Heinrich, R., and Schuster, S. (1996) *The Regulation of Cellular Systems*, Chapman & Hall, New York
14. Westerhoff, H. V., Groen, A. K., and Wanders, R. J. (1984) Modern theories of metabolic control and their applications (review). *Biosci. Rep.* **4,** 1–22 CrossRef Medline
15. Westerhoff, H. V., and Chen, Y. D. (1984) How do enzyme activities control metabolite concentrations? An additional theorem in the theory of metabolic control. *Eur. J. Biochem.* **142,** 425–430 CrossRef Medline
16. Achcar, F., Kerkhoven, E. J., SilicoTryp Consortium, Bakker, B. M., Barrett, M. P., and Breitling, R. (2012) Dynamic modelling under uncertainty: the case of *Trypanosoma brucei* energy metabolism. *PLoS Comput. Biol.* **8,** e1002352 CrossRef Medline
17. Liberti, M. V., Dai, Z., Wardell, S. E., Baccile, J. A., Liu, X., Gao, X., Baldi, R., Mehrmohamadi, M., Johnson, M. O., Madhukar, N. S., Shestov, A. A., Chio, I. I. C., Elemento, O., Rathmell, J. C., Schroeder, F. C., *et al.* (2017) A predictive model for selective targeting of the Warburg effect through GAPDH inhibition with a natural product. *Cell Metab.* **26,** 648–659.e8 CrossRef Medline
18. Bakker, B. M., Mensonides, F. I., Teusink, B., van Hoek, P., Michels, P. A., and Westerhoff, H. V. (2000) Compartmentation protects trypanosomes from the dangerous design of glycolysis. *Proc. Natl. Acad. Sci. U.S.A.* **97,** 2087–2092 CrossRef Medline
19. Shestov, A. A., Liu, X., Ser, Z., Cluntun, A. A., Hung, Y. P., Huang, L., Kim, D., Le, A., Yellen, G., Albeck, J. G., and Locasale, J. W. (2014) Quantitative determinants of aerobic glycolysis identify flux through the enzyme GAPDH as a limiting step. *Elife* **3,** CrossRef 10.7554/eLife.03342 Medline
20. Groen, A. K., van Roermund, C. W., Vervoorn, R. C., and Tager, J. M. (1986) Control of gluconeogenesis in rat liver cells: flux control coefficients of the enzymes in the gluconeogenic pathway in the absence and presence of glucagon. *Biochem. J.* **237,** 379–389 CrossRef Medline
21. Page, R. A., Okada, S., and Harwood, J. L. (1994) Acetyl-CoA carboxylase exerts strong flux control over lipid synthesis in plants. *Biochim. Biophys. Acta* **1210,** 369–372 CrossRef Medline
22. Fell, D. A. (1992) Metabolic control analysis: a survey of its theoretical and experimental development. *Biochem. J.* **286,** 313–330 CrossRef Medline
23. Cascante, M., Boros, L. G., Comin-Anduix, B., de Atauri, P., Centelles, J. J., and Lee, P. W. (2002) Metabolic control analysis in drug discovery and disease. *Nat. Biotechnol.* **20,** 243–249 CrossRef Medline
24. Reznik, E., Christodoulou, D., Goldford, J. E., Briars, E., Sauer, U., Segrè, D., and Noor, E. (2017) Genome-scale architecture of small molecule regulatory networks and the fundamental trade-off between regulation and enzymatic activity. *Cell Rep.* **20,** 2666–2677 CrossRef Medline
25. Bakker, B. M., Michels, P. A., Opperdoes, F. R., and Westerhoff, H. V. (1999) What controls glycolysis in bloodstream form *Trypanosoma brucei*? *J. Biol. Chem.* **274,** 14551–14559 CrossRef Medline
26. Qian, H., and Beard, D. A. (2005) Thermodynamics of stoichiometric biochemical networks in living systems far from equilibrium. *Biophys. Chem.* **114,** 213–220 CrossRef Medline
27. Beard, D. A., and Qian, H. (2007) Relationship between thermodynamic driving force and one-way fluxes in reversible processes. *PLoS One* **2,** e144 CrossRef Medline
28. Noor, E., Flamholz, A., Liebermeister, W., Bar-Even, A., and Milo, R. (2013) A note on the kinetics of enzyme action: a decomposition that highlights thermodynamic effects. *FEBS Lett.* **587,** 2772–2777 CrossRef Medline
29. Bennett, B. D., Kimball, E. H., Gao, M., Osterhout, R., Van Dien, S. J., and Rabinowitz, J. D. (2009) Absolute metabolite concentrations and implied enzyme active site occupancy in *Escherichia coli*. *Nat. Chem. Biol.* **5,** 593–599 CrossRef Medline
30. Park, J. O., Rubin, S. A., Xu, Y. F., Amador-Noguez, D., Fan, J., Shlomi, T., and Rabinowitz, J. D. (2016) Metabolite concentrations, fluxes and free energies imply efficient enzyme usage. *Nat. Chem. Biol.* **12,** 482–489 CrossRef Medline
31. Westerhoff, H. V., Plomp, P. J., Groen, A. K., and Wanders, R. J. (1987) Thermodynamics of the control of metabolism. *Cell Biophys.* **11,** 239–267 CrossRef Medline
32. Van Dam, K., Westerhoff, H. V., Krab, K., van der Meer, R., and Arents, J. C. (1980) Relationship between chemiosomotic flows and thermodynamic forces in oxidative phosphorylation. *Biochim. Biophys. Acta* **591,** 240–250 CrossRef Medline
33. Liebermeister, W. (2013) Elasticity sampling links thermodynamics to metabolic control. arXiv:1309.0267
34. Noor, E., Bar-Even, A., Flamholz, A., Reznik, E., Liebermeister, W., and Milo, R. (2014) Pathway thermodynamics highlights kinetic obstacles in central metabolism. *PLoS Comput. Biol.* **10,** e1003483 CrossRef Medline
35. Bassham, J. A., and Krause, G. H. (1969) Free energy changes and metabolic regulation in steady-state photosynthetic carbon reduction. *Biochim. Biophys. Acta* **189,** 207–221 CrossRef Medline
36. Yasumasu, I., Asami, K., Shoger, R. L., and Fujiwara, A. (1973) Glycolysis of sea urchin eggs: rate-limiting steps and activation at fertilization. *Exp. Cell Res.* **80,** 361–371 CrossRef Medline
37. Possemato, R., Marks, K. M., Shaul, Y. D., Pacold, M. E., Kim, D., Birsoy, K., Sethumadhavan, S., Woo, H. K., Jang, H. G., Jha, A. K., Chen, W. W., Barrett, F. G., Stransky, N., Tsun, Z. Y., Cowley, G. S., *et al.* (2011) Functional genomics reveal that the serine synthesis pathway is essential in breast cancer. *Nature* **476,** 346–350 CrossRef Medline
38. Xie, J., Dai, C., and Hu, X. (2016) Evidence that does not support pyruvate kinase M2 (PKM2)-catalyzed reaction as a rate-limiting step in cancer cell glycolysis. *J. Biol. Chem.* **291,** 8987–8999 CrossRef Medline
39. Moreno-Sánchez, R., Saavedra, E., Rodríguez-Enríquez, S., and Olín-Sandoval, V. (2008) Metabolic control analysis: a tool for designing strategies to manipulate metabolic pathways. *J. Biomed. Biotechnol.* **2008**, 597913 Medline
40. Shelley, M. D., Autenrieth, R. L., Wild, J. R., and Dale, B. E. (1996) Thermodynamic analysis of trinitrotoluene biodegradation and mineralization pathways. *Biotechnol. Bioeng.* **51,** 198–205 CrossRef Medline
41. Kummel, A., Panke, S., and Heinemann, M. (2006) Putative regulatory sites unraveled by network-embedded thermodynamic analysis of metabolome data. *Mol. Syst. Biol.* **2,** 2006.0034 CrossRef Medline
42. Locasale, J. W. (2018) New concepts in feedback regulation of glucose metabolism. *Curr. Opin. Syst. Biol.* **8,** 32–38 CrossRef
43. Reid, M. A., Dai, Z., and Locasale, J. W. (2017) The impact of cellular metabolism on chromatin dynamics and epigenetics. *Nat. Cell Biol.* **19,** 1298–1306 CrossRef Medline

44. Brown, G. C., Hafner, R. P., and Brand, M. D. (1990) A "top-down" approach to the determination of control coefficients in metabolic control theory. *Eur. J. Biochem.* **188,** 321–325 CrossRef Medline
45. Chelliah, V., Juty, N., Ajmera, I., Ali, R., Dumousseau, M., Glont, M., Hucka, M., Jalowicki, G., Keating, S., Knight-Schrijver, V., Lloret-Villas, A., Natarajan, K. N., Pettit, J.-B., Rodriguez, N., Schubert, M., *et al.* (2015) BioModels: ten-year anniversary. *Nucleic Acids Res.* **43,** D542–D548 CrossRef Medline
46. Sauro, H. M., Hucka, M., Finney, A., Wellock, C., Bolouri, H., Doyle, J., and Kitano, H. (2003) Next generation simulation tools: the Systems Biology Workbench and BioSPICE integration. *OMICS* **7,** 355–372 CrossRef Medline

Thermodynamic constraints on the regulation of metabolic fluxes

Ziwei Dai and Jason W. Locasale

J. Biol. Chem. 2018, 293:19725-19739.
doi: 10.1074/jbc.RA118.004372 originally published online October 25, 2018